size, and signal acquisition capability. Given certain constraints on all these variables, probe weights were evaluated as a function of R_p (the closest approach of the spacecraft to the planet). This relationship is shown in the final report[1] for the case of a single probe, $\gamma_E = -20°$, $P = 50$ bars, and shows that as R_p increases the probe weight increases. The range (and signal loss) also increases and thus a larger transmitter is required, causing increases in the thermal-structural weight.

Probe weight vs entry angle

Another aspect of the communications geometry is γ_E, which affects both range and probe aspect angle. However, the power requirements did not prove to be a significant factor in the probe weight and in fact the transmitter size decreased at the steeper entry angle for the 300 bar design because of the shorter range at the end of the mission. The probe weights are shown in the final report,[1] with design pressure as a parameter.

The probe's thermal design is affected by entry angle variation through the resultant variation in the structural supports carrying the entry loads from the aeroshell to the probe's internal equipment. As the entry angle increases, the cross-sectional area of the supports increases and therefore the heat transfer into the probe (during descent) increases. These supports represent the major heat leak into the probe through the multilayer insulation. They are designed to minimize heat conduction by making them out of titanium and installing them at 30°, which doubles their conduction path. The impact of entry angle on the thermal design, however, is overshadowed by the very large weight increases in the aeroshell and heat shield, due to the higher dynamic pressures and heating rates.

Conclusions

The thermal control objective in this study was to determine the system penalties resulting from thermal protection requirements of probes descending as deep as 1000 bars. The configuration tradeoff study showed that the relatively low pressure and temperature environment favored the exposed pressure shell with multilayer insulation, and the relatively high pressure and temperature environment favored the use of both external and internal insulation with a pressure shell. In the former case, it means a strong dependence on seals, the possibility of thermal stresses in the shell, and an inefficient application for multilayer. In the latter case the performance of the exposed insulation is critical not only to the payload temperature but to the shell where high temperatures mean lower mechanical properties and an accentuated high pressure seal problem. Until it is demonstrated that payload components are compatible with high pressures, little gain can be expected from the alternative configuration designs. There is a strong need for performance data on insulations in these applications and environments before realistic thermal-structural designs can be postulated for Jovian atmospheric probes.

References

[1] "Jupiter Atmospheric Entry Mission Study—Final Report," MCR-71-1, March 1971, Martin Marietta Corp., Denver, Colo.

[2] Carroll, P. C., "A Jupiter Atmospheric Entry Mission," AIAA Paper 71-832, Denver, Colo., 1971.

[3] Ranz, W. E. and Marshall, W. R., "Evaporation from Drops," *Chemical Engineering Progress*, Vol. 48, 1952, pp. 141–146, 173–180.

[4] "1975 Venus Multiprobe Mission Study—Final Report," MCR-70-89, April 1970, Martin Marietta Corp., Denver Colo.

[5] "Delta-Class Venus Probe Mission Study—Final Report," AVSD-0433-60-RR, Oct. 1969, Avco Systems Div., Wilmington, Mass.

Subsonic, Transonic, and Supersonic Nozzle Flow by the Inverse Technique

DAVID J. NORTON*
Texas A&M University, College Station, Texas

Nomenclature

A,B,C = centerline velocity constants
a = acoustic velocity
b = stretching function constant
c_p = specific heat, constant pressure
C_D = nozzle mass flow coefficient
F = isentropic constant
H = enthalpy
P = pressure
q = Velocity vector
r,θ,z = cylindrical coordinates
T = temperature
u,v,w = cylindrical velocities
γ = specific heat ratio
ε_c = contraction ratio
ξ = axial stretched coordinate
ρ = density
ψ = streamline, stream function

Subscripts and Superscripts

o = stagnation condition
t = throat
cl = centerline
$*$ = sonic value
1-D = one dimensional

Introduction

TWO-dimensional calculations for nozzles and wind tunnel have usually been treated in three distinct regimes: the subsonic, the transonic, and the supersonic. Since we have a powerful tool for the solution of hyperbolic equations in the Method of Characteristics (MOC), the supersonic flow has received a great deal of attention. Flow solutions by MOC are initiated in the transonic region from an initial data surface which is a Cauchy boundary condition. At first, MOC calculations employed one-dimensional results for this initial data. However, special transonic analyses have now been derived reflecting to some degree the two-dimensional effects at the throat.[1–4] The subsonic flow which leads up to the throat has been largely ignored due to the difficulty of treating the elliptic problem. The classical method of solution of elliptic equations requires boundary conditions of the Neumann or Dirichlet type over a closed region. The solution for the interior points is effected by relaxation allowing the prescribed boundary conditions to determine the interior values. In gasdynamic flows, often these boundary conditions are not known; in fact, these conditions are often the primary purpose of the analysis. This is especially true of the transonic region boundary conditions which are useful for MOC supersonic flow solutions. Thus, it is difficult to treat each flow regime separately and the flow in a mixed region must be solved.

At the present time there are three methods for handling these flows: the Asymptotic Time Method, the Error minimization Technique, and the Inverse Cauchy Technique. The first makes use of the unsteady flow equations which are hyperbolic with respect to time.[5] This method has been shown feasible for flows initiated from an infinite reservoir where the initial velocities are zero. However, for flows originating

Received August 12, 1971; revision received January 24, 1972. This work was supported by NASA while author was on duty at JPL.

Index categories: Subsonic and Transonic Flow; Nozzle and Channel Flow.

* Assistant Professor, Aerospace Engineering. Member AIAA.

from a constant area duct, it is necessary to solve the unsteady flowfield many times to obtain the proper initial conditions to prevent instabilities. The large number of resultant calculations influence the accuracy due to roundoff errors. The Error Minimization Technique[6] uses a sophisticated relaxation scheme which tends to remove errors from the transonic region. This method tends to be time consuming and to exhibit convergence problems in the chamber, although agreement with experiment at the throat is good.

Inverse Method

Recently, there has been some attempts to obtain a mathematically and physically consistent solution of the flowfield in a nozzle from the mass generation surface through the supersonic region. This approach is necessary for such problems as the prediction of heat transfer in nozzles with rapidly converging inlets and low radius of curvature throat sections, as well as, the calculation of throat solutions including the effects of the subsonic geometry. The method employes an assumed centerline function which is of the Cauchy type in that the values and the derivatives of the function are known.[7] For arbitrarily specified centerline data, the solution of the governing flow equations may not exist, and if it does, it may not depend continuously on the data. However, if analytic data is specified, the Cauchy-Kowalewsky theorem[8] indicates that a solution exists in the neighborhood of the initial data. Integration is initiated at the centerline and is continued radially in the half-plane indefinitely, providing instabilities do not develop. End conditions may be specified, but these may not be of the Cauchy type since these would overspecify the solution unless they are imposed at $x = \pm\infty$. However, boundary condition of Dirichlet or Neumann type are permissible at any x. This permits the postulation of rotational types of flow in the sense that entropy may vary normal to the streamlines due to nonuniformities in the combustion or due to tangential velocities.

Analysis

In this section the governing gasdynamic equations for rotational (nonhomentropic), steady flow are presented. Subsequently, these equations will be transformed into the ψ,ξ plane which represents, respectively, the streamline function and a stretched axial coordinate.

Continuity equation

$$\partial\psi/\partial r = \rho w r;\ \partial\psi/\partial z = -\rho u r \tag{1}$$

Momentum equations

$$\partial p/\partial r = -\rho(u\,\partial u/\partial r + w\,\partial u/\partial z - v^2/r) \tag{2}$$

$$\partial p/\partial z = -\rho(u\,\partial w/\partial r + w\,\partial w/\partial z) \tag{3}$$

$$D(vr)/Dt = u\,\partial(vr)/\partial r + w\,\partial(vr)/\partial z = 0 \tag{4}$$

Energy equation

$$\bar{q}\cdot\nabla H_0 = 0 \tag{5}$$

The momentum equations are those of Euler for axisymmetric flow and they include swirling flow. The energy equation is equivalent to the process equation and it assures constant total enthalpy and entropy along streamlines.

Since the equations are to be solved numerically, and it is well-known that the Cauchy boundary conditions can give rise to numerical instabilities if not properly handled,[9] it was decided to transform the governing equations into a form which puts any geometry into a rectangular shape and which spaces the network of interior points more finely in regions of the greatest gradients of the dependent variables. The transformation is formally stated as

$$r, z \rightarrow \psi(r, z), \xi(z) \tag{6}$$

The results of the Jacobian yield the partials of the old independent variables in terms of the new ones

$$\begin{aligned} &\partial r/\partial\psi = (\rho r w)^{-1};\ \partial z/\partial\psi = 0 \\ &\partial r/\partial\xi = (u/w\xi');\ \partial z/\partial\xi = dz/d\xi = 1/\xi' \end{aligned} \tag{7}$$

Using the preceding results the governing equations become

$$\partial r/\partial\psi = 1/\rho r w \tag{8}$$

$$\partial r/\partial\xi = u/w\xi' \tag{9}$$

$$\frac{\partial P}{\partial\psi} = \frac{1}{wr}\left[-w\frac{\partial u}{\partial\xi}\xi' + \frac{\Gamma(\psi)^2}{r^3}\right] \tag{10}$$

$$P = F(\psi)\rho^{\gamma} \tag{11}$$

$$\Gamma = \Gamma(\psi) = vr = \text{const on } \psi \tag{12}$$

$$H_0 = H_0(\psi) = c_p T + \tfrac{1}{2}(u^2 + v^2 + w^2) \tag{13}$$

In general $F(\psi)$, $H_0(\psi)$, $\Gamma(\psi)$ are determined from the chamber conditions.

Nozzle Flow Analysis

To solve a nozzle flow problem in the transformed plane using the inverse technique an analytic function then centerline velocity must be specified which contains the salient features of the nozzle to be designed. In addition, a stretching fuction ξ must be chosen. The following functions were employed:

$$\xi = 1 + \tanh[b(z - z_t)] \tag{14}$$

$$\bar{w}_{cl} = w/_{cl}a^* = 1 + A/2\{\tanh[B(z - z_t)] + \tanh[C(z - z_t)]\} \tag{15}$$

The stretching function maps the physical x direction between 0 and 2 with the sonic velocity, on the centerline, at 1. The centerline velocity function has three arbitrary constants which control ε_c, R_c/R_t, and θ_w. At $z = z_t$ the centerline velocity function is unity with a maximum slope. The constant A control the contraction ratio by specifying the initial

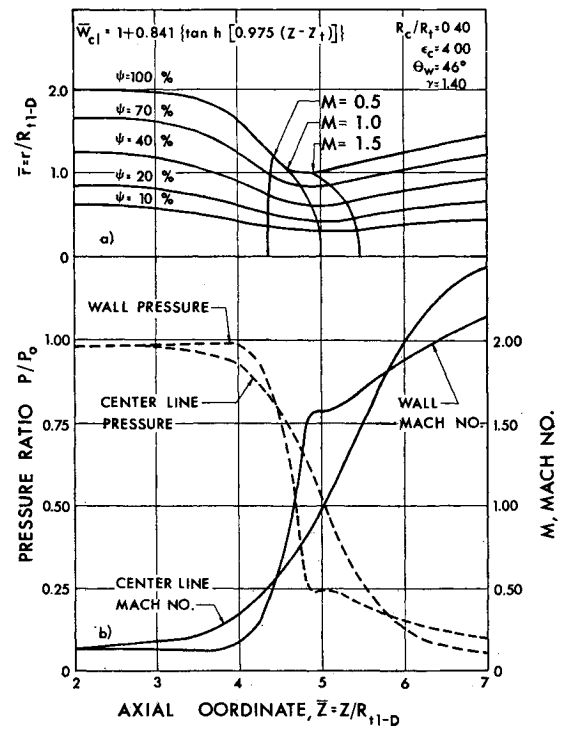

Fig. 1 Nozzle contour and property variations at the centerline and wall for a nozzle with $\gamma = 1.40$, $\varepsilon_c = 4.0$, and $R_c/R_t = 0.40$.

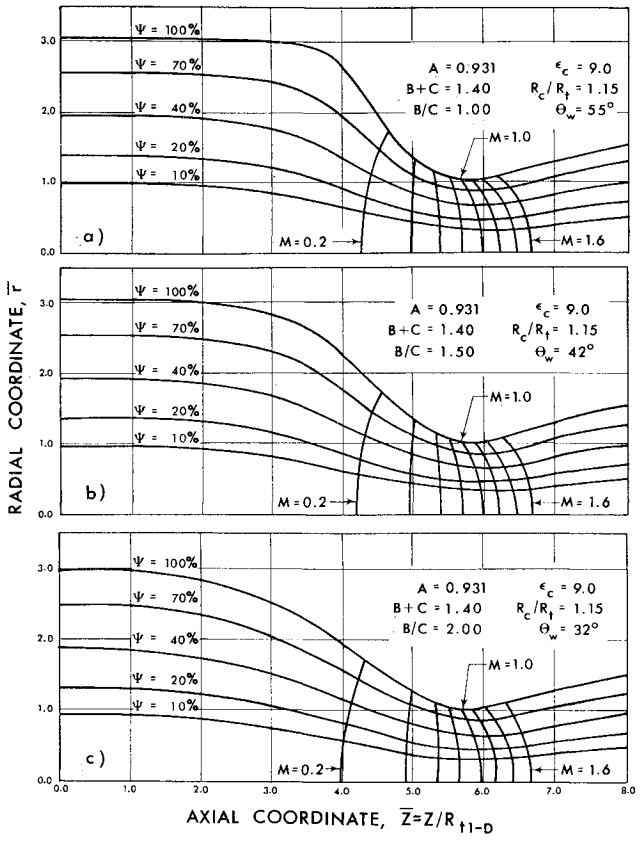

Fig. 2 The effect of the ratio of B/C in varying θ_w for given ε_c, and R_c/R_t.

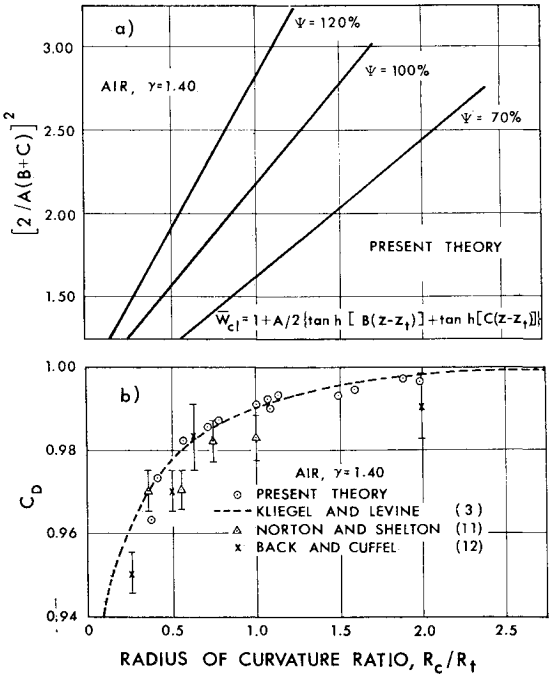

Fig. 3 The correlating parameter $[2/A(B+C)]^2$ and the nozzle discharge coefficient as a function of R_c/R_t.

velocity. The constants B and C control the radius of curvature for a given ε_c. Then θ_w is determined by the streamline and a complicated function of A, B, and C. (For a more complete discussion the centerline velocity function or numerical methods see Ref. 10.)

Figure 1a presents the results for a given centerline velocity function integrated in the half-space above the centerline. Any streamline may represent a nozzle wall in the inviscid sense. Also shown are the lines of constant Mach number. In Fig. 1b the wall and centerline, pressures and Mach numbers are shown for the same case. Note the retardation of the wall Mach number at the nozzle inlet and just after the tight throat section. The former effect leads to boundary-layer separation, while the latter can cause shocks in the nozzle expansion.

Figure 2 illustrates the use of the arbitrary constants B and C for a given A. In this example $\varepsilon_c = 9.0$, $R_c/R_t = 1.15$ for the three nozzles while θ_w varies from 55° to 32°. Figure 3a presents the relationship between R_c/R_t and a correlating parameter $[2/A(B+C)]^2$ for various values of ψ. These curves result from a number of calculations and permit choice of the centerline function for a given design. Figure 3b illustrates the results for C_D compared to R_c/R_t. Note that the results are in general agreement with the theory of Ref. 3 for $R_c/R_t > 0.5$. Also, the present theory is generally above but within the range of the experimental results.

Conclusions

The inverse technique permits solution of the entire nozzle problem using the complete gasdynamic equations including rotational effects. The contours generated are analytic, hence they do not match existing contours, although the key features such as ε_c, R_c/R_t, and θ_w can be included. Solutions, with plots, require approximately two minutes of Univac 1108 time for a given centerline velocity function. It should be emphasized that the inverse method is not suited to the detailed prediction of an existing nozzle contours. Since the centerline velocity function and the streamlines are analytic, they cannot match exactly nozzles designed from combinations of simple geometric shapes. However, if the walls are constructed along solution streamlines the flow in the interior is known.

References

[1] Sauer, R., "General Characteristics of the Flow through Nozzles at near Critical Speeds," TM 1147, 1947, NACA.

[2] Hall, I. M., "Transonic Flow in Two-Dimensional and Axially-Symmetric Nozzles," *Quarterly Journal of Mechanics and Applied Mathematics*, Vol. XV, 1962, pp. 487–508.

[3] Kliegel, J. D. and Levine, J. N., "Transonic Flow in Small Throat Radius of Curvature Nozzles," *AIAA Journal*, Vol. 7, No. 7, July 1969, pp. 1375–1378.

[4] Hopkins, D. F. and Hill, D. E., "Effect of Small Radius of Curvature on Transonic Flow in Axisymmetric Nozzles," *AIAA Journal*, Vol. 4, No. 8, Aug, 1966, pp. 1337–1343.

[5] Migdal, D., Klein, K., and Moretti, G., "Time-Dependent Calculations for Transonic Nozzle Flow," *AIAA Journal*, Vol. 7, No. 2, Feb. 1969, pp. 372–373.

[6] Prozan, R. J. and Kooker, D. E., "The Error Minimization Technique with Application to a Transonic Nozzle Solution," *Journal Fluid Mechanics*, Vol. 43, Pt. 2, 1970, pp. 269–277.

[7] Pirumov, U. G., "Calculation of the Flow in a Laval Nozzle," *Soviet Physics-Doklady*, Vol. 12, No. 9, March 1968, pp. 857–860.

[8] Hardamard, J., *Lectures on Cauchy's Problem in Partial Differential Equations*, Dover, New York, 1952.

[9] Frank, L. S., "Difference Methods for Solving the Improper Cauchy Problem Simulating Flow of a Perfect Gas Through a Nozzle," *Soviet Physics-Doklady*, Vol. 13, No. 9, March 1969, pp. 856–858.

[10] Norton, D. J., "Subsonic, Transonic, and Supersonic Nozzle Flow by the Inverse Technique," Aerospace Engineering Dept., Rept. AED-R71-10, July 1971, Texas A&M University, College Station, Texas.

[11] Norton, D. J. and Shelton, S., "Performance of Rocket Nozzles with Low Radius of Curvature Rations," *JPL Space Programs Summary* 37-55, Vol. III, Feb. 1969, Pasadena, Calif., pp. 167–169.

[12] Back, L. H. and Cuffel, R. F., "Flow Coefficients for Supersonic Nozzles with Comparatively Small Radius of Curvature Throat, *Journal of Spacecraft and Rockets*, Vol. 8, No. 2, Feb. 1971, pp. 196–198.